https://doi.org/10.33108/visnyk_tntu
Scientific Journal of the Ternopil National Technical University
2025, № 3 (119) https://doi.org/10.33108/visnyk_tntu2025.03
ISSN 2522-4433. Web:

UDC 004.9:006.3

INFORMATION TECHNOLOGY FOR PREDICTING THE HYSTERESIS BEHAVIOR OF SHAPE MEMORY ALLOYS BASED ON A STACKING ENSEMBLE MACHINE LEARNING MODEL

Dmytro Tymoshchuk; Oleh Yasniy

Ternopil Ivan Puluj National Technical University,
Ternopil, Ukraine

Shape Memory Alloys are characterized by a nonlinear hysteretic behavior on the stress–strain (σ–ε) diagram, where the loop area determines the amount of energy dissipated per cycle. In this work, an ensemble Stacking machine learning model was developed to predict the hysteresis behavior of SMAs under cyclic loading at different frequencies (0.5, 1, 3, and 5 Hz). The model was constructed using experimental data from 100–250 loading cycles. Random Forest, Gradient Boosting, Extra Trees, k-Nearest Neighbors (kNN), Support Vector Regression (SVR), and Multilayer Perceptron (MLP) were employed as base algorithms. The ElasticNet model was selected as the meta-learner and tuned using GridSearchCV with GroupKFold validation. This approach ensured the combination of ensemble stability with adaptive selection of the most informative predictions from the base models. The obtained results showed a high accuracy in reproducing the stress–strain relationship: $R^2 > 0.995$, MSE < 0.0007, MAE < 0.02, and MAPE < 1.3 % on the test data. Validation on independent cycles 251 and 300 confirmed the model's generalization ability, achieving $R^2 > 0.974$, MSE < 0.007, MAE < 0.06, and MAPE < 4.8 %. The interpretability of the model was provided by the SHAP method, which quantitatively determines the contribution of each input feature to the prediction. It was found that Stress is the dominant factor influencing the prediction, while UpDown defines the loading–unloading phase, and Cycle reflects the accumulation of cyclic effects. The developed ensemble Stacking model is an integral component of an information technology framework for predicting the hysteresis behavior of shape memory alloys using machine learning methods. The proposed approach provides not only high prediction accuracy but also a physically grounded interpretability of the results.

SMA; hysteresis; machine learning; ensemble model; Stacking Regressor; ElasticNet; Explainable AI (XAI); SHAP analysis; strain prediction; information technology.

https://doi.org/10.33108/visnyk_tntu2025.03.134 *Received 15.09.2025*

1. INTRODUCTION

Intelligent materials capable of adaptively responding to changing external conditions form the foundation for the development of modern structures with controllable properties. Among them, Shape Memory Alloys (SMAs) occupy a special place. They are distinguished by two unique properties: the shape memory effect (SME) and superelasticity (SE). These characteristics arise from reversible martensitic–austenitic phase transformations that occur at the microstructural level under the influence of temperature or mechanical loading. As a result, the material can not only recover its original shape after deformation but also withstand significant mechanical loads without permanent changes in geometry. The combination of high elasticity, durability, and self-recovery capability has led to a wide range of SMA applications across various engineering fields [1–5].

The stress-strain diagram of an SMA exhibits a pronounced hysteretic behavior. During a loading–unloading cycle, a closed loop is formed on the stress–strain (σ–ε) diagram, representing the reversible martensitic–austenitic transformations within the material. The area enclosed by this loop quantitatively corresponds to the energy dissipated per cycle, E_{diss} and is calculated as follows:

$$E_{diss} = \int_{\varepsilon_{min}}^{\varepsilon_{max}} \big(\sigma_1(\varepsilon) - \sigma_2(\varepsilon)\big) d\varepsilon, \quad (1)$$

where σ is the stress (MPa), ε is the strain (dimensionless), $\sigma_1(\varepsilon)$ and $\sigma_2(\varepsilon)$ represent the loading and unloading stages of the same cycle, respectively.

This characteristic determines the material's ability to damp mechanical vibrations and serves as an important parameter in evaluating its functional properties. The geometry of the hysteresis loop and the amount of dissipated energy are governed by a combination of thermokinetic and operational parameters of the material. The key factors include the start and finish temperatures of the martensitic transformation (M_s, M_f) and the reverse austenitic transformation (A_s, A_f). The frequency of the applied load f (Hz) also has a significant influence. Furthermore, the shape of the hysteresis loop evolves with an increasing number of loading–unloading cycles N.

The frequency of the applied external load is one of the key factors determining the functional properties of SMAs [6–7]. It is particularly significant when the material operates under repeated cyclic loading, during which martensitic–austenitic transformations are periodically activated. The loading frequency directly affects the thermal processes within the material. At higher frequencies, self-heating of the specimen may occur, leading to a local temperature rise, a shift in the phase transformation temperature ranges, and consequently, a partial loss of functionality. Moreover, frequency is a decisive factor shaping the hysteretic behavior of SMAs. As the frequency increases, the geometry of the stress–strain loop changes, directly influencing its area and, therefore, the amount of energy dissipated per cycle. High frequencies cause the loop to narrow and reduce its energy capacity due to incomplete phase transformations, whereas low frequencies promote a more complete development of both martensitic and austenitic phases. Accurate reproduction of the nonlinear hysteretic behavior of shape memory alloys under varying loading frequencies is essential for designing durable and reliable components in aerospace, biomedical, and robotic systems. However, classical analytical models often fail to achieve sufficient agreement with experimental data, which justifies the use of modern machine learning methods. Machine learning algorithms can effectively capture complex nonlinear relationships between stress, strain, loading frequency, number of cycles, and other operational parameters. Consequently, the application of machine learning enables higher accuracy in predicting hysteresis behavior. Furthermore, integrating Explainable AI (XAI) methods [8] allows for interpreting the influence of individual input features on the output, increasing model transparency and providing deeper insights into the physical processes underlying SMA behavior.

The review paper [9] emphasizes that Shape Memory Alloys (SMAs) are widely used in sensors, actuators, aerospace engineering, medicine, and robotics; however, their nonlinear behavior complicates the application of traditional numerical modeling methods. The authors note that the use of artificial intelligence approaches is a promising direction, as they can reduce computational costs and improve prediction accuracy. Considerable attention is given to artificial neural networks (ANNs), which are employed to model the properties of SMAs in various forms – such as wires, reverse-spring wires, rods, rings, and porous materials. The review summarizes the current neural network architectures and training methods and confirms their strong potential for engineering and biomedical applications.

In the study [10], there was proposed an interpretable machine learning approach for predicting the martensitic transformation peak temperature (Tp) in high-entropy shape memory alloys (HESMAs) based on the TiZrHfNiCoCu system. The authors constructed a dataset, performed feature selection, and developed a model that achieved an error of less than 3% for newly synthesized alloys. The model was interpreted using SHAP analysis, which revealed the

key role of the CV22 feature (Allred–Rochow electronegativity). The analysis also showed that higher concentrations of Co and Cu have a positive effect on Tp, thus enabling the guided design of HESMAs with tailored transformation temperatures.

The study [11] investigated the use of machine learning methods to predict phase transformation temperatures in high-temperature shape memory alloys (HTSMAs) based on titanium. The authors compared the performance of three algorithms: Artificial Neural Networks (ANN), Support Vector Regression (SVR), and Random Forest Regression (RFR). These models were applied to determine the austenite finish temperature, the martensite start temperature, and the thermal hysteresis. The ANN provided the most accurate predictions for the austenite finish temperature, while the SVR achieved the highest accuracy for the martensite start temperature. The RFR model produced the most precise estimation of hysteresis derived from the predicted transformation temperatures. The analysis of feature importance confirmed the significant role of Pt and Ni in the phase transformations, which is consistent with previous research. The study demonstrated the potential of machine learning to accelerate the design of titanium-based HTSMAs with predictable temperature-dependent behavior.

The study [12] proposed a physics-informed machine learning approach for predicting the martensitic transformation start temperature in HESMAs. The authors expanded the existing HESMA database and performed prediction using the Extremely Randomized Trees algorithm with two strategies. The first strategy considered only the alloy composition, while the second included a set of physical descriptors such as mixing enthalpy, atomic radius, and electronegativity. The second approach achieved higher prediction accuracy. Experimental validation on six synthesized alloys confirmed the reliability of the developed model. In addition, the authors implemented a design tool for HESMAs aimed at achieving M_s values above 400°C.

The study [13] employed several machine learning models, including linear regression, Random Forest, and Support Vector Regression, to predict the parameters of the monoclinic B19` lattice phase in two datasets: ZrO_2-based shape memory ceramics and NiTi-based high-entropy SMAs. The results showed that linear regression provided the most accurate predictions for the parameters a_c, a_m, b_m, and c_m in NiTi-based HESMAs, while Random Forest achieved the best predictions for β_m in both datasets. In contrast, the SVR model exhibited the largest deviations from the experimental values. The combination of Random Forest and linear regression improved the accuracy of estimating martensitic phase parameters across different SMA materials, showing promise for their use in high-temperature applications.

The article [14] explored the use of machine learning methods for rapid prediction of the martensitic transformation start temperature (M_s) in shape memory alloys. The Gradient Boosting algorithm achieved the highest accuracy with $R^2 = 0.92$ and MAE = 23.42 °C. The combination of correlation analysis, recursive feature elimination, and exhaustive search identified six key factors, while SHAP-based interpretation provided a clear understanding of feature importance distribution. To address the challenge of low M_s values in NiTi alloys, the concept of high-entropy alloys was integrated into the modeling process. The model predicted the composition $Ti_{19}Zr_{19}Hf_{19}Ni_{37}Cu_6$ with an M_s above 400 °C, confirming the effectiveness of the proposed approach for extending the operational temperature range of SMAs.

The aim of this study is to develop an ensemble Stacking machine learning model for predicting the hysteretic behavior of SMAs under repeated cyclic loading at different frequencies and to evaluate its accuracy using experimental data. The research also involves the application of Explainable Artificial Intelligence (XAI) methods to interpret the behavior of the constructed model, perform a quantitative analysis of the contribution of input variables to the prediction, and identify the dominant factors that determine the evolution of the hysteresis loop during repeated loading cycles. This approach is intended not only to achieve high prediction accuracy but also to enhance the interpretability of the results, thereby contributing to a deeper understanding of the physical mechanisms governing the behavior of SMAs.

2. MATERIAL AND METHODS

To construct the dataset for training and testing the machine learning models, experimental data were used from fatigue tests of a NiTi shape memory alloy (SMA) wire with a diameter of 1.5 mm and a length of 210 mm [15]. The experiments were conducted at room temperature using a servo-hydraulic testing machine STM-100. The chemical composition of the alloy consisted of 55.78% Ni and 44.12% Ti, with the total content of impurities (Co, Cu, Cr, Fe, Nb, C, H, O, N) not exceeding 0.04%.

The dataset included the following input features: material stress σ (MPa), cycle number N corresponding to the loading–unloading sequence, and an indicator specifying the loading or unloading stage. The output variable was the material strain ε (%) which characterizes the response of the NiTi alloy to the applied stress under different loading frequencies f (0.5, 1, 3, and 5 Hz). In this study, experimental data from 100 to 250 loading-unloading cycles of the SMA were used.

The number of data samples corresponding to each loading frequency is presented in Table 1.

Table 1

Number of data samples for different loading frequencies

Frequency, Hz	0.5	1	3	5
Number of samples	3,051	16,006	18,573	14,949

The formation of the training and test datasets was performed using the GroupShuffleSplit method from Python. This method provides a random split of the data into training and test subsets while preserving the group membership of observations. In this study, the group index was represented by the loading cycle number N, which prevents data from the same cycle from appearing simultaneously in both subsets. The data were divided into an 80/20 ratio, with 80% of the records used for training and 20% reserved for independent testing to evaluate the model's generalization capability.

Based on the prepared subsets, an ensemble model of the Stacking Regressor type [16] was constructed. Ensemble learning through stacking combines several base models to enhance the predictive system's generalization ability. Unlike bagging or boosting, stacking is not limited to a single model type and allows the combination of algorithms of different nature, forming a multi-level architecture. The base models included Random Forest [17], Gradient Boosting [18], Extra Trees [19], K-Nearest Neighbors (kNN) [20], Support Vector Regressor (SVR) [21], and Multilayer Perceptron (MLP) [22]. The last three models were implemented within a Pipeline using StandardScaler for feature normalization. The ElasticNet algorithm [23] was used as the meta-model, combining the properties of Lasso and Ridge regularization. Optimal hyperparameters were determined using GridSearchCV with the evaluation metric neg_mean_squared_error. Reliable model assessment within loading cycles was ensured by a custom GroupKFoldWithGroups wrapper (n_splits = 5), which considers the grouped structure of the data during cross-validation.

In general form, the prediction of the ensemble Stacking model was defined as a linear combination of the predictions of the base models:

$$\bar{y} = b + \sum_{j=1}^{m} w_j . \bar{y}_j, \tag{2}$$

where $\bar{y}$ is the final ensemble prediction, $\bar{y}_j$ is the prediction of the j-th base model, w_j is the weight assigned by the ElasticNet meta-model, b is the bias term, and m is the number of base models.

The coefficients w_j represent the contribution of each base model to the overall ensemble prediction. The bias term b is an independent model parameter that defines the baseline level of the predicted variable and allows adjustment of the model output mean when all input features are zero. The inclusion of this parameter ensures a shift of the prediction hyperplane relative to the origin, compensating for systematic deviations of the base models and improving the accuracy of the overall approximation.

To evaluate the performance of the ensemble model, classical regression metrics were used to characterize the accuracy and consistency of predictions with experimental data [24]. The Mean Squared Error (MSE) reflects the average squared difference between predicted and actual values. Since it is sensitive to large deviations, this metric is particularly effective for assessing models where minimizing significant errors is crucial. The Mean Absolute Error (MAE) measures the average absolute difference between predicted and actual values, regardless of the error direction. This metric provides an interpretable measure of the average prediction error expressed in the same units as the target variable. The Coefficient of Determination (R^2) indicates the proportion of the variance in the target variable that is explained by the model. A value of R^2 close to 1 signifies a high level of agreement between the predictions and experimental data, whereas a low value indicates an insufficient ability of the model to reproduce the observed relationships. The Mean Absolute Percentage Error (MAPE) represents the average percentage deviation of the prediction from the actual values. It is convenient for comparing model performance across different datasets because it expresses errors in percentage form and allows accuracy to be interpreted in relative terms. Overall, these metrics provided a comprehensive evaluation of the ensemble model's effectiveness, considering both the accuracy of data reproduction and the model's stability on the independent test set.

To enhance the interpretability of the ensemble model results, the SHapley Additive exPlanations (SHAP) method was applied. This approach is based on Shapley game theory and provides a quantitative assessment of the contribution of each input feature to the model's prediction [25]. SHAP analysis makes it possible to interpret both the global influence of features on the model (the average importance of each feature across all observations) and the local contribution of individual variables to a specific prediction. This enables a clear explanation of why the model produced a particular output and helps identify the key factors that determine the hysteretic behavior of shape memory alloys under repeated cyclic loading conditions.

3. RESULTS AND DISCUSSION

For the quantitative analysis of the weights of the base models within the Stacking ensemble, an ElasticNet regressor was used as the meta-model. This algorithm combines the properties of L1 (Lasso) and L2 (Ridge) regularization. Such an approach provides a balance between selecting the most informative models through the sparsity effect of the L1 norm and stabilizing their weights through the L2 component, which helps prevent overfitting and excessive correlation among the base model predictions. During training, a five-fold group cross-validation (GroupKFold) was performed with respect to the cycle numbers, ensuring independence between the training and validation subsets.

The hyperparameter tuning process using GridSearchCV identified the optimal values of α and l_1_ratio, which minimized the mean squared error in

cross-validation. The value α = 0.01 resulted in mild regularization, sufficient to prevent overfitting without significantly reducing accuracy. This setting is particularly important for ensemble models, where base predictors may exhibit partial correlation with each other.

The parameter l_1 ratio ∈ [0, 1] defines the balance between L1 and L2 regularization in the overall penalty function. When l_1 ratio = 1, the model uses pure Lasso (L1) regularization, which promotes sparsity by setting insignificant coefficients to zero. This helps selecting the most influential features or, in the case of an ensemble, the most significant base models. When l_1 ratio = 0, the model applies pure Ridge (L2) regularization, which does not eliminate coefficients but reduces their amplitudes, stabilizing the model in the presence of multicollinearity. The intermediate value l_1 ratio = 0.8 combines the effects of both methods: the L1 component performs partial selection of the most relevant models, while the L2 component ensures robustness to noise and redundant or correlated base predictors.

The normalized distribution of ElasticNet meta-model weights represents the relative contribution of each base algorithm to the ensemble's final prediction. The weights were normalized so that the sum of their absolute values was equal to one, allowing for a direct comparison of the influence of different models. Figure 1 illustrates the variation in weight structure across four loading frequencies, showing how the contribution of individual algorithms evolves with increasing deformation frequency in the SMA.

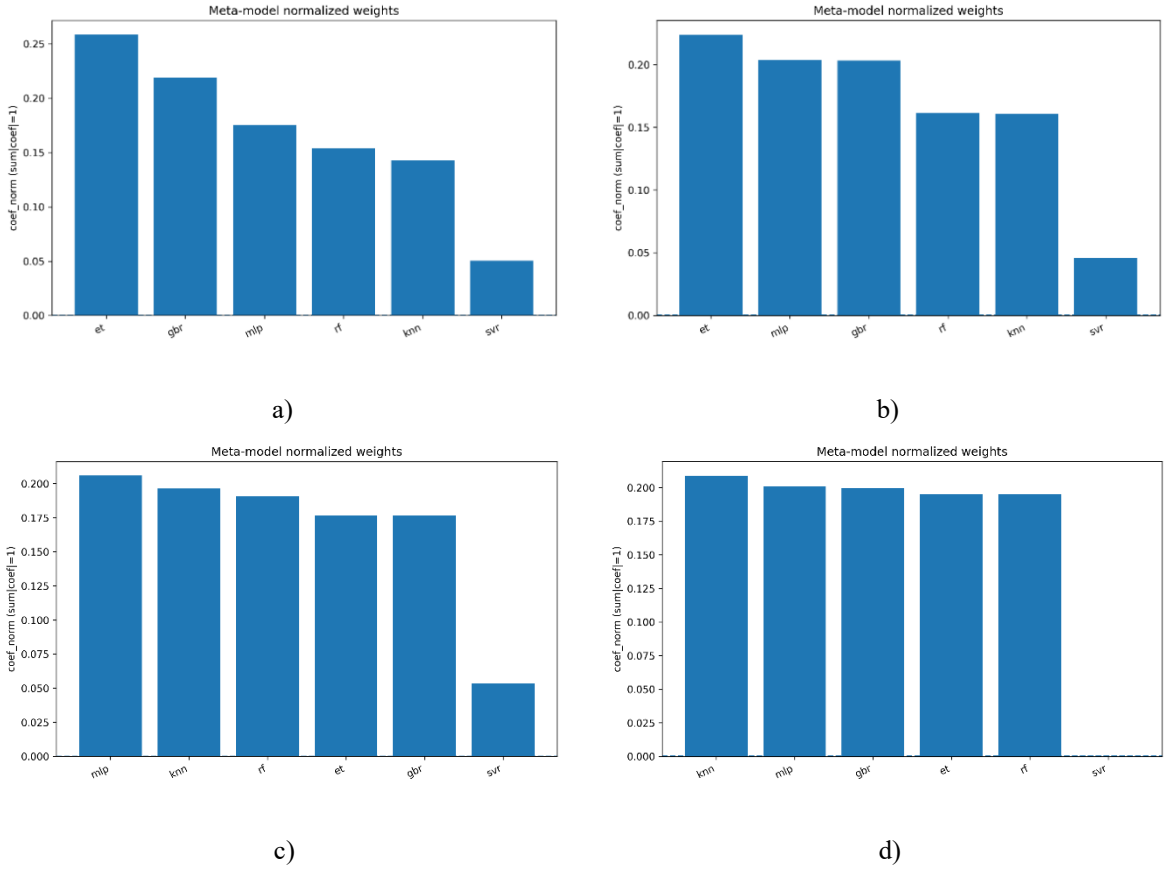

Figure 1. Normalized weights of the ElasticNet meta-model for the base regressors: 0.5 Hz (a), 1 Hz (b), 3 (c) Hz, 5 Hz (d)

At the low loading frequency of 0.5 Hz (Fig. 1 a), the highest weights were assigned to the ExtraTrees and Gradient Boosting models, indicating the dominant contribution of

tree-based ensembles to the overall prediction. When the frequency increased to 1 Hz (Fig. 1 b), the contribution of the MLP model became more significant, gradually gaining a larger share of the ensemble. A further increase to 3 Hz (Fig. 1 c) was accompanied by a noticeable strengthening of the MLP and kNN models, while the influence of tree-based algorithms gradually decreased. At the maximum frequency of 5 Hz (Fig. 1 d), the weights were distributed almost uniformly among all base models, and the weight of the SVR dropped to a value close to zero. Thus, in all examined frequency regimes, the SVR consistently had the smallest impact on the meta-prediction, whereas the leading role was alternately played by tree-based ensembles, MLP, or kNN models, depending on the cyclic loading frequency.

The performance of the developed ensemble model was evaluated using standard regression metrics, namely the mean squared error (MSE), mean absolute error (MAE), coefficient of determination (R^2), and mean absolute percentage error (MAPE). These indicators were calculated both for the test dataset within the training cycle range (100–250) and for independent experimental cycles (251 and 300) that were not used during training, validation, or testing. The quantitative evaluation results are summarized in Table 1.

Table 1

Prediction errors of the ensemble Stacking model for different loading frequencies and cycles.

Cycle type	Frequency (Hz)	MSE	MAE	R^2	MAPE
Test	0.5	0.0004	0.0163	0.9992	0.0057
	1	0.0004	0.0175	0.9990	0.0075
	3	0.0007	0.0218	0.9976	0.0106
	5	0.0006	0.0218	0.9959	0.0125
Independent (251)	0.5	0.0004	0.0167	0.9992	0.0059
	1	0.0003	0.0155	0.9992	0.0068
	3	0.0012	0.0287	0.9970	0.0146
	5	0.0011	0.0274	0.9952	0.0155
Independent (300)	0.5	0.0015	0.0339	0.9969	0.0116
	1	0.0006	0.0203	0.9987	0.0078
	3	0.0019	0.0360	0.9957	0.0169
	5	0.0071	0.0622	0.9741	0.0479

For the test data within the training cycle range (100–250), the obtained error values were exceptionally low, confirming the high performance of the developed Stacking model. The mean squared error (MSE) did not exceed 0.0007, the mean absolute error (MAE) was approximately 0.02, and the mean absolute percentage error (MAPE) remained below 1.3%. The coefficient of determination ($R^2 > 0.995$) in all cases indicates that the ensemble accurately reproduces the functional relationship between stress and strain. For the independent verification cycles, a slight but consistent decrease in accuracy was observed with increasing loading frequency and cycle number. For the 251st cycle, the R^2 value remained nearly unchanged (≈ 0.99 for 0.5 – 1 Hz), and MAPE did not exceed 1.6%. In the 300th cycle, the prediction error increased slightly. At 3 Hz, MAE reached 0.036 and MAPE was approximately 1.7%, while at 5 Hz a more noticeable deviation was

observed (MSE = 0.0071, R^2 = 0.974, MAPE ≈ 4.8%). Overall, the results show that the ensemble maintains high stability and accuracy across the entire frequency range, with errors remaining within acceptable limits even beyond the training cycles. This confirms the model's strong generalization ability and its capability to correctly capture the complex nonlinear behavior of SMAs under repeated loading.

The distribution of the prediction residuals for the test dataset is shown in Figure 2.

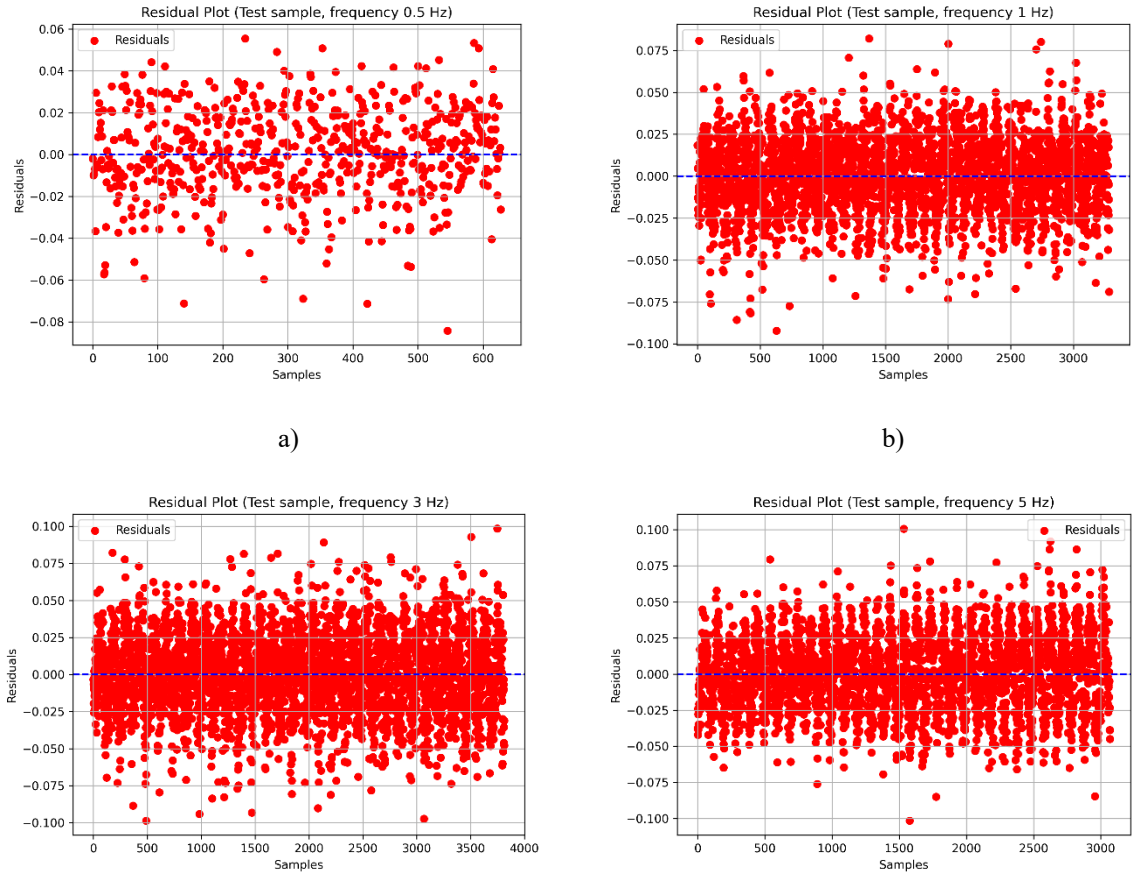

Figure 2. Distribution of prediction residuals of the Stacking model for the test datasets at different loading frequencies: 0.5 Hz (a), 1 Hz (b), 3 Hz (c), 5 Hz (d)

In all cases, the residuals were uniformly distributed around the horizontal axis, showing no noticeable systematic bias in the predictions of the ElasticNet meta-model. For the frequencies of 0.5 and 1 Hz, the point cloud appeared nearly symmetrical, and the residual variation range was within ±0.07, confirming the high accuracy and stability of the ensemble. At 3 and 5 Hz, a slight increase in the spread of residuals up to ±0.1 was observed; however, their distribution remained random without any pronounced autocorrelation. This indicates that the model accurately reproduces nonlinear dependencies even under dynamic loading conditions and at higher rates of martensitic–austenitic phase transformations. The absence of a cone-shaped pattern or displacement of the residual cloud from the horizontal axis confirms the constant nature of error variance and the uniform quality of prediction across the entire dataset.

The developed ensemble Stacking model successfully reproduced the hysteretic behavior of the SMA during cyclic loading. Based on the input parameters: material

stress σ (MPa), cycle number N, corresponding to the loading–unloading process, and the loading phase indicator the model predicts the instantaneous strain value ε (%). This enables not only the estimation of individual points but also the reconstruction of the complete σ–ε, hysteresis loop, which characterizes the phase transformations between martensite and austenite.

Figure 3 presents the reconstructed hysteresis loops for cycles 251 and 300 at a loading frequency of 1 Hz.

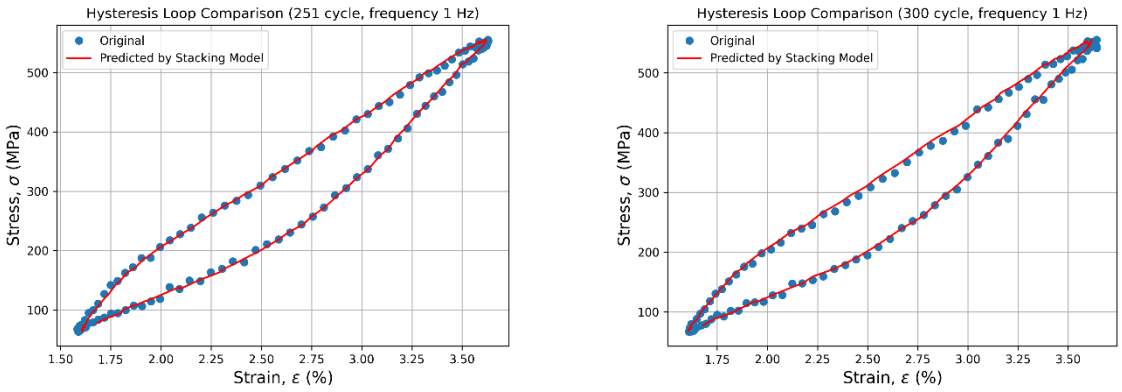

a) b)

Figure 3. Comparison of experimental and predicted hysteresis loops: 251st cycle (a), 300th cycle (b)

The reconstructed dependencies showed a high level of agreement between the experimental data and the predictions of the Stacking model. For the 251st cycle (Fig. 3a), the curves almost completely overlap, indicating high prediction accuracy during both loading and unloading phases. The model accurately reproduces the key regions of the hysteresis behavior, particularly the characteristic nonlinear response during the martensitic and austenitic phase transformations. For the 300th cycle (Fig. 3b), the shape of the hysteresis loop is also reproduced with high precision, although small discrepancies between the predicted and experimental data can be observed in the form of slight deviations. These differences are consistent with the obtained statistical error metrics (Table 1). Despite these minor variations, the overall loop contour, its width, and slope in the transformation regions are accurately captured. Overall, the results obtained demonstrate strong consistency between the predicted and experimental hysteresis loops and confirm the model's ability to generalize to unseen cycles. This validates the effectiveness of the ensemble approach in describing the nonlinear hysteretic behavior of SMAs.

To interpret the behavior of the ensemble Stacking model, the SHAP method was applied. This technique enables a quantitative assessment of the contribution of each input feature to the final prediction. Belonging to the class of XAI methods, SHAP explains the results of machine learning models without compromising prediction accuracy. The analysis was performed using KernelExplainer, which approximates local feature influences in nonlinear models. To reduce computational complexity, the sample was limited to a subset of 400 background data points derived from the training set. The evaluation was conducted for the features Stress, Cycle, and UpDown.

The results of the global SHAP analysis are presented in Figure 4, which shows the mean absolute SHAP values for all features in the test dataset.

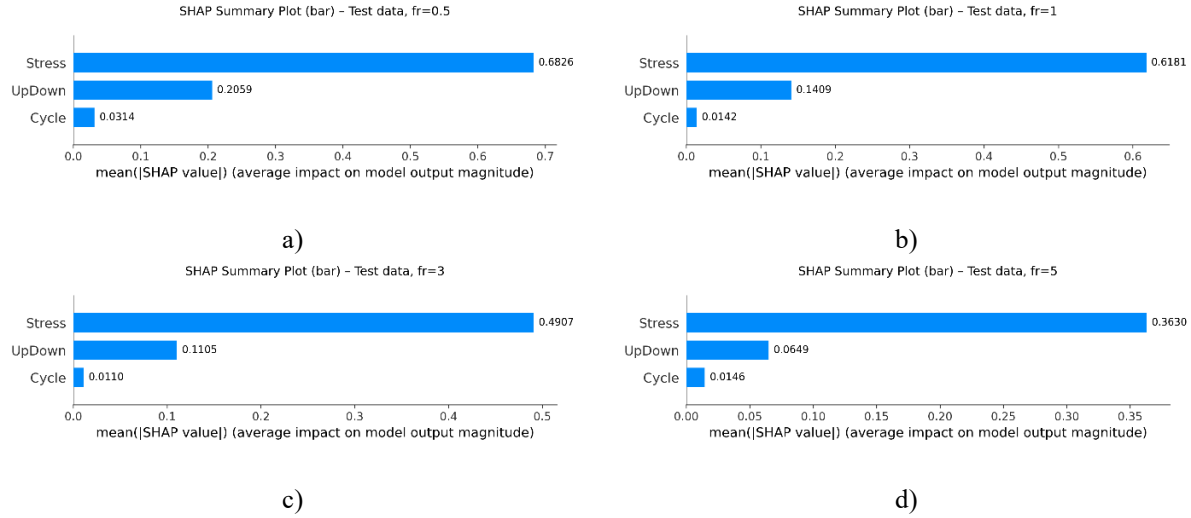

Figure 4. Global mean absolute SHAP values for the test datasets at different loading frequencies: 0.5 Hz (a), 1 Hz (b), 3 Hz (c), 5 Hz (d)

The variable Stress has the strongest influence on the model's prediction, confirming its primary role in determining the strain behavior of the SMA. The large SHAP values associated with this feature indicate that even small variations in stress have a significant effect on the predicted strain. The second most important factor is UpDown, which represents the loading or unloading stage, that is, the direction of movement within the hysteresis loop. Its contribution shows that the model effectively distinguishes between the different phases of the loading cycle. The influence of the Cycle feature is comparatively smaller, although it increases for later cycles, as illustrated in Figure 5.

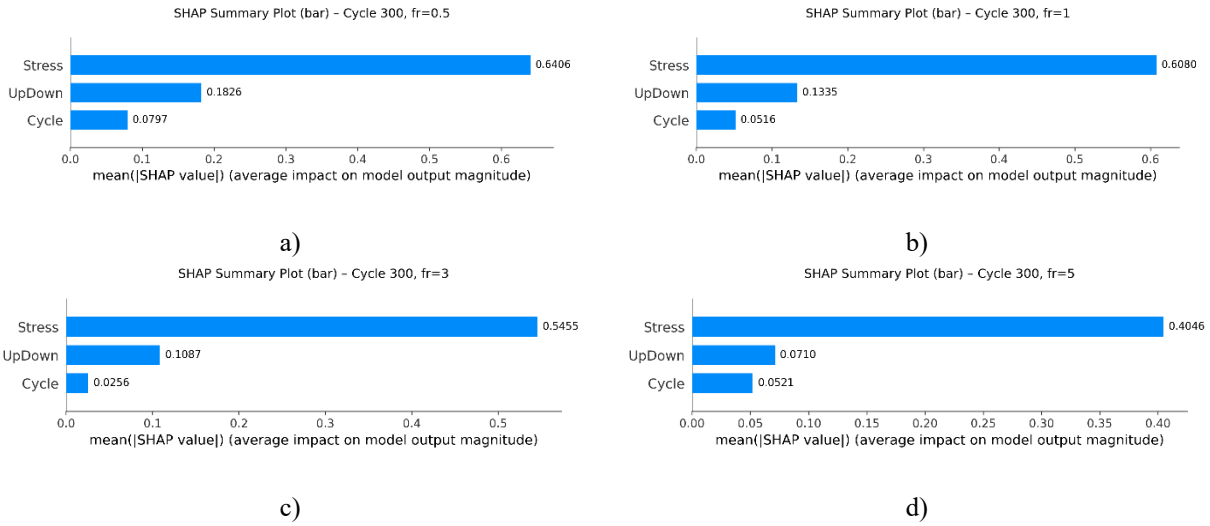

Figure 5. Global mean absolute SHAP values for the 300th cycle at different loading frequencies: 0.5 Hz (a), 1 Hz (b), 3 Hz (c), 5 Hz (d)

A local SHAP analysis for an individual sample (the 45th measurement of the 300th cycle at a loading frequency of 1 Hz) is presented in Figure 6.

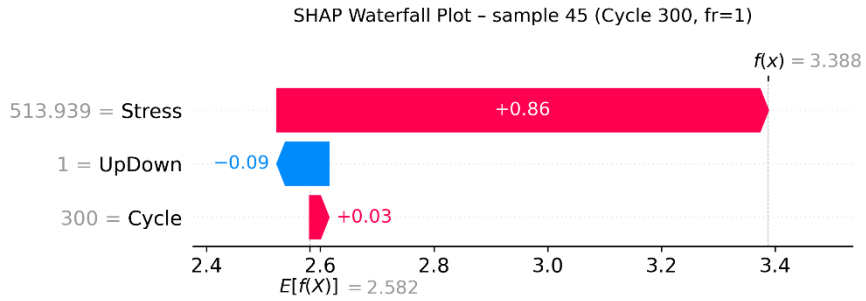

Figure 6. Local SHAP Waterfall Plot for the 45th measurement of the 300th cycle at a loading frequency of 1 Hz.

The largest positive contribution to the predicted value comes from Stress (+0.86), confirming the dominant role of mechanical loading in material deformation. The feature UpDown = 1, corresponding to the loading phase, exerts a minor negative influence (–0.09), slightly reducing the predicted strain during this stage. The variable Cycle = 300 provides a small positive contribution (+0.03).

The model's initial expected value, $E[f(\mathrm{X})] = 2.582$, shifts to the final prediction $f(x)$=3.388 under the influence of these factors, which align well with the experimental observations. Thus, the local SHAP analysis shows that increasing stress is the primary factor driving strain growth, while the loading phase and cycle number act as secondary corrective parameters that influence the shape of the hysteresis loop.

The obtained results indicate that the ensemble Stacking model not only reproduces the nonlinear mechanical behavior of the material with high accuracy but also preserves a physically interpretable structure of dependencies. The application of SHAP analysis quantitatively confirmed the dominant role of stress in shaping the deformation behavior of the NiTi alloy and revealed the influence of cyclic effects responsible for the evolution of the hysteresis loop during repeated loading.

The developed ensemble Stacking model represents a component of an information technology framework for predicting the hysteretic behavior of SMAs using machine learning methods. The proposed framework covers the full data analysis cycle, from the preprocessing of experimental measurements to the modeling of complex nonlinear relationships and the subsequent interpretation of results using XAI approaches. This integration ensures not only high accuracy in reproducing hysteresis loops but also provides a physically grounded explanation of each parameter's contribution, making the model suitable for practical applications in assessing the durability and performance of SMAs.

4. CONCLUSIONS

An ensemble Stacking model was developed in this study to predict the hysteretic behavior of NiTi shape memory alloys (NiTi-SMA) under cyclic loading at frequenciesof 0.5, 1, 3, and 5 Hz. The model showed high accuracy on the test data within the 100–250 cycle range, achieving $R^2 > 0.995$, MSE < 0.0007, MAE < 0.02, and MAPE < 1.3%. Validation on cycles 251 and 300 confirmed its strong generalization capability. The most noticeable decrease in prediction accuracy occurred at 5 Hz for the 300th cycle; however, the results remained acceptable ($R^2 \approx 0.974$). The application of Explainable AI SHAP methods provided an interpretable understanding of the contribution of input parameters and confirmed the physical consistency of the model's operation, highlighting the dominant influence of stress and the role of loading cycles in shaping the hysteresis loop. Future research will focus on advancing the proposed information technology framework for predicting the hysteretic behavior of shape memory alloys

by integrating recurrent neural network architectures such as Bidirectional LSTM and GRU, which are expected to further enhance prediction accuracy.

References

1. Sharma K., & Srinivas G. (2020Flying smart: Smart materials used in aviation industry. Materials Today: Proceedings, 27, pp. 244–250. https://doi.org/10.1016/j.matpr.2019.10.115
2. Niu X., Yao X., & Dong E. (2025) Design and control of bio-inspired joints for legged robots driven by shape memory alloy wires. Biomimetics, 10 (6), pp. 378. https://doi.org/10.3390/biomimetics10060378
3. Schmelter T., Bade L., & Kuhlenkötter B. (2024) A two-finger gripper actuated by shape memory alloy for applications in automation technology with minimized installation space. Actuators, 13 (10), p. 425. https://doi.org/10.3390/act13100425
4. Riccio A., Sellitto A., Ameduri S., Concilio A., & Arena M. (2021). Shape memory alloys (SMA) for automotive applications and challenges. In Shape Memory Alloy Engineering, pp. 785–808. Elsevier. https://doi.org/10.1016/B978-0-12-819264-1.00024-8
5. Zhang H., Zhao L., Li A., & Xu S. (2024) Design and hysteretic performance analysis of a novel multi-layer self-centering damper with shape memory alloy. Buildings, 14 (2), p. 483. https://doi.org/10.3390/buildings14020483
6. Iasnii V., Krechkovska H., Budz V., Student O., & Lapusta Y. (2024). Frequency effect on low-cycle fatigue behavior of pseudoelastic NiTi alloy. Fatigue & Fracture of Engineering Materials & Structures. https://doi.org/10.1111/ffe.14331
7. Tymoshchuk D., Yasniy O., Maruschak P., Iasnii V., & Didych I. (2024) Loading Frequency Classification in Shape Memory Alloys: A Machine Learning Approach. Computers, 13 (12), p. 339. https://doi.org/10.3390/computers13120339
8. IBM. (n.d.-b). What is Explainable AI (XAI)? | IBM. https://www.ibm.com/think/topics/explainable-ai.
9. Hmede R., Chapelle F., & Lapusta Y. (2022) Review of neural network modeling of shape memory alloys. Sensors, 22 (15), p. 5610. https://doi.org/10.3390/s22155610
10. He S., Wang Y., Zhang Z., Xiao F., Zuo S., Zhou Y., Cai X., & Jin X. (2023) Interpretable machine learning workflow for evaluation of the transformation temperatures of TiZrHfNiCoCu high entropy shape memory alloys. Materials & Design, 225, 111513. https://doi.org/10.1016/j.matdes.2022.111513
11. Sridharan S., Velayutham R., Behera S., & Murugesan J. (2025). Machine Learning-Based Temperature-Induced Phase Transformation Temperature Prediction of Ti-Based High-Temperature Shape Memory Alloy. Journal of Materials Engineering and Performance. https://doi.org/10.1007/s11665-025-11236-z
12. Thiercelin L., Peltier L., & Meraghni F. (2024) Physics-informed machine learning prediction of the martensitic transformation temperature for the design of “NiTi-like” high entropy shape memory alloys. Computational Materials Science, 231, 112578. https://doi.org/10.1016/j.commatsci.2023.112578
13. Lam T.-N., Jiang J., Hsu M.-C., Tsai S.-R., Luo M.-Y., Hsu S.-T., Lee W.-J., Chen C.-H., & Huang E.-W. (2024) Predictions of Lattice Parameters in NiTi High-Entropy Shape-Memory Alloys Using Different Machine Learning Models. Materials, 17 (19), 4754. https://doi.org/10.3390/ma17194754
14. Liu C., & Su H. (2024) Machine learning aided prediction of martensite transformation temperature of NiTi-based shape memory alloy. Materials Today Communications, 41, 110720. https://doi.org/10.1016/j.mtcomm.2024.110720
15. Iasnii V., Bykiv N., Yasniy O., & Budz V. (2022) Methodology and some results of studying the influence of frequency on functional properties of pseudoelastic SMA. Scientific journal of the Ternopil national technical university, 107 (3), pp. 45–50. https://doi.org/10.33108/visnyk_tntu2022.03.045
16. StackingRegressor. (n.d.). Available at: https://scikit-learn.org/stable/modules/generated/sklearn.ensemble.StackingRegressor.html.
17. RandomForestRegressor. (n.d.). Available at: https://scikit-learn.org/stable/modules/generated/sklearn.ensemble.RandomForestRegressor.html.
18. Clark B., & Lee F. (n.d.). What is Gradient Boosting? | IBM. Available at: https://www.ibm.com/think/topics/gradient-boosting.
19. ExtraTreesRegressor. (n.d.). Retrieved from Available at: https://scikit-learn.org/stable/modules/generated/sklearn.ensemble.ExtraTreesRegressor.html.
20. Nearest Neighbors. (n.d.). Available at: https://scikit-learn.org/stable/modules/neighbors.html.
21. Support Vector Machines. (n.d.). Available at: https://scikit-learn.org/stable/modules/svm.html.
22. Haykin S. (2009). Neural networks and learning machines (3rd ed.). Hamilton, ON, Canada: Prentice Hall.
23. ElasticNet. (n.d.). Available at: https://scikit-learn.org/stable/modules/generated/sklearn.linear_model.ElasticNet.html.
24. Metrics and scoring: quantifying the quality of predictions. (n.d.). Available at: https://scikit-learn.org/stable/modules/model_evaluation.html#model-evaluation.
25. GitHub – shap/shap: A game theoretic approach to explain the output of any machine learning model. (n.d.-b).

Available at: https://github.com/shap/shap.

УДК 004.9:006.3

ІНФОРМАЦІЙНА ТЕХНОЛОГІЯ ПРОГНОЗУВАННЯ ГІСТЕРЕЗИСНОЇ ПОВЕДІНКИ СПЛАВІВ З ПАМ'ЯТТЮ ФОРМИ НА ОСНОВІ АНСАМБЛЕВОЇ STACKING-МОДЕЛІ МАШИННОГО НАВЧАННЯ

Дмитро Тимощук; Олег Ясній

Тернопільський національний технічний університет імені Івана Пулюя, Тернопіль, Україна

Резюме. *Сплави з пам'яттю форми (СПФ) характеризуються нелінійною гістерезисною поведінкою на діаграмі деформування (σ–ε), площа петлі якої визначає енергію, розсіяну за цикл. Запропоновано ансамблеву Stacking-модель машинного навчання для прогнозування гістерезисної поведінки СПФ за умов циклічного навантаження з різними частотами (0,5; 1; 3 та 5 Гц). Для побудови моделі використано експериментальні дані 100–250 циклів навантаження. У якості базових алгоритмів застосовано Random Forest, Gradient Boosting, Extra Trees, kNN, SVR та MLP. За метамодель вибрано ElasticNet, яку налаштовано за допомогою GridSearchCV з GroupKFold-валідацією. Такий підхід забезпечив поєднання стабільності ансамблю з адаптивним відбором найінформативніших прогнозів базових моделей. Отримані результати показали високу точність відтворення залежності напруження-деформація. Для тестових даних $R^2 > 0{,}995$, MSE < 0,0007, MAE < 0,02, MAPE < 1,3 %. Перевірка на незалежних циклах 251 та 300 підтвердила узагальнювальну здатність моделі, зокрема $R^2 > 0{,}974$, MSE < 0,007, MAE < 0,06, MAPE < 4.8 %. Інтерпретованість моделі забезпечено методом SHAP, який кількісно визначає внесок кожної вхідної ознаки у формування прогнозу. Встановлено, що Stress є головним чинником формування прогнозу, тоді як ознака UpDown визначає фазу навантаження-розвантаження, а Cycle відображає накопичення циклічних ефектів. Розроблена ансамблева Stacking-модель є складовою інформаційної технології прогнозування гістерезисної поведінки сплавів з пам'яттю форми із застосуванням методів машинного навчання. Запропонований підхід забезпечує не лише високу точність прогнозування, але й фізично обґрунтовану інтерпретованість результатів.*

Ключові слова: *SMA, гістерезис, машинне навчання, ансамблева модель, Stacking Regressor, ElasticNet, Explainable AI (XAI), SHAP-аналіз, прогнозування деформації, циклічне навантаження.*

https://doi.org/10.33108/visnyk_tntu2025.03.134 *Отримано 15.09.2025*